A BGK-Penalization-Based Asymptotic-Preserving Scheme for the Multispecies Boltzmann Equation

Shi Jin,[1,2,3] **Qin Li**[4]

[1] *Department of Mathematics, Shanghai Jiao Tong University, Shanghai 200240, China*

[2] *Institute of Natural Sciences, Shanghai Jiao Tong University, Shanghai 200240, China*

[3] *Ministry of Education Key Lab of Scientific and Engineering Computing, Shanghai Jiau Tong University, Shanghai 200240, China*

[4] *Department of Mathematics, University of Wisconsin-Madison, Madison, Wisconsin 53706*

Received 23 October 2011; accepted 12 July 2012
Published online 10 September 2012 in Wiley Online Library (wileyonlinelibrary.com).
DOI 10.1002/num.21746

An asymptotic-preserving (AP) scheme is efficient in solving multiscale problems where kinetic and hydrodynamic regimes coexist. In this article, we extend the BGK-penalization-based AP scheme, originally introduced by Filbet and Jin for the single species Boltzmann equation (Filbet and Jin, J Comput Phys 229 (2010) 7625–7648), to its multispecies counterpart. For the multispecies Boltzmann equation, the new difficulties arise due to: (1) the breaking down of the conservation laws for each species and (2) different convergence rates to equilibria for different species in disparate masses systems. To resolve these issues, we find a suitable penalty function—the local Maxwellian that is based on the mean velocity and mean temperature and justify various asymptotic properties of this method. This AP scheme does not contain any nonlinear nonlocal implicit solver, yet it can capture the fluid dynamic limit with time step and mesh size independent of the Knudsen number. Numerical examples demonstrate the correct asymptotic-behavior of the scheme. Numer Methods Partial Differential Eq 29: 1056–1080, 2013

Keywords: asymptotic-preserving schemes; multispecies Boltzmann equations; fluid dynamic limit

I. INTRODUCTION

In kinetic theory, the Boltzmann equation is a fundamental equation to describe the evolution of rarefied gases. In this article, we are interested in numerical solution of the Boltzmann equation for multispecies gas mixture. The most basic example is high-altitude gas, which could be modeled as a binary mixture of oxygen and nitrogen. Other applications of gas mixture may come from nuclear engineering or evaporation–condensation.

Correspondence to: Shi Jin, Department of Mathematics, University of Wisconsin-Madison, Madison, WI 53706 (e-mail: jin@math.wisc.edu)
Contract grant sponsor: NSF; contract grant number: DMS-1114546
Contract grant sponsor: NSF RNMS grant DMS-1107291

One of the difficulties in numerically solving the Boltzmann equation comes from the varying Knudsen number, which describes the ratio of the mean free path over a typical length scale such as the domain size. If the Knudsen number is small, the collision term becomes numerically stiff. When using an explicit scheme, to guarantee the numerical stability, one has to resolve the small Knudsen number to avoid instability, and this causes a tremendous computational cost. On the other hand, it is very difficult to use implicit schemes because of the nonlinear and the nonlocal nature of the collision operator.

The Chapman-Enskog expansion for the Boltzmann equation yields the compressible Euler or Navier–Stokes equations in the limit of vanishing Knudsen number. Generally speaking, numerically solving the hydrodynamic system is much more efficient, so when the Knudsen number is small, one can just solve this set of equations in lower dimension. However, in zones where these macroscopic models break down, one has to come back to solve the Boltzmann equation. This domain decomposition approach has attracted a great amount of attentions [1–10]. The main difficulty there is to determine the matching interface conditions between two different domains in which different physical models are used.

Another approach, the one we are going to pursue in this article, is called the asymptotic-preserving (AP) method. This method dates back to the 90s from the last century and has been widely used in time-dependent kinetic and hyperbolic systems since then. This approach looks for simple and cheap solvers for the Boltzmann equation that can preserve asymptotic limits from the microscopic to the macroscopic models in the discrete setting, which means that the numerical solution to the Boltzmann equation should converge to that of the Euler equations when the Knudsen number vanishes. Compared with multiphysics domain decomposition methods, this framework only solves one set of equation: the microscopic one. In the hydrodynamic regime, it becomes a robust hydrodynamic solver "automatically" without resolving the small Knudsen number or switching to the macroscopic model. As summarized by Jin [11], an AP scheme for kinetic equations should have the following features:

- it preserves the discrete analogy of the Chapman-Enskog expansion, namely, it is a suitable scheme for the kinetic equation, yet, when holding the mesh size and time step fixed and letting the Knudsen number go to zero, the scheme becomes a suitable scheme for the limiting fluid dynamic Euler equations;
- implicit collision terms can be implemented efficiently.

There are several variations of the AP property, including weakly AP, relaxed-AP, and strongly AP, defined as follows (see [12] and also a recent review [13]):

- *weakly AP*. If the data are within $O(\varepsilon)$ of the local equilibrium initially, they remain so for all future time steps;
- *relaxed AP*. For nonequilibrium initial data, the solution will be projected to the local equilibrium beyond an initial layer (after several time steps).
- *strongly AP*. For nonequilibrium initial data, the solution will be projected to the local equilibrium immediately in one time step.

In general, the strongly AP property is preferred and was the designing principle of most of the classical AP schemes [14, 15]. The relaxed-AP is a concept introduced recently in [12], which was shown numerically to be sufficient to capture the hydrodynamic limit when the Knudsen number goes to zero. The weakly AP is often a necessary condition for the AP property. Many non-AP schemes do not satisfy this property, namely solutions initially close to the local equilibrium can move away. See discussion in [12].

Several AP schemes have recently been designed for the Boltzmann equation for monospecies. One approach was to use the micro–macro decomposition method [16] (see its multispecies extension in [17]), but the issue of designing an efficient implicit collision term, which is necessary for numerical stability independent of the Knudsen number, is still unsolved. An earlier approach introduced by Gabetta et al., [18] uses the truncated Wild Sum for uniform numerical stability of the collision term. For a simple BGK model, it was realized by Coron and Perthame in [19] that an implicit BGK operator can be integrated explicitly, using the basic conservation properties of the BGK operator. Utilizing this property, Filbet and Jin [12] introduced the BGK penalization method for the Boltzmann collision operator. The main idea is to subtract the Boltzmann operator by a BGK operator and then add the BGK operator back. Only the latter, BGK operator is treated implicitly, whereas the complicated Boltzmann operator is solved explicitly. The entire scheme is implemented explicitly, yet the numerical stability is independent of the Knudsen number, and the relaxed AP property was achieved (which was verified numerically). Yan and Jin recently extended this approach to a positive and strongly AP scheme by adding in an extra relaxation step [20]. This BGK penalization idea, in the space homogeneous case, agrees with the Wild Sum approach [18], but they differ when the space is inhomogeneous. Another implementations can be found using the exponential Runge–Kutta method, see Dimarco and Pareschi [21], resulting a strongly AP scheme with positivity. A rigorous justification of the AP property of this methodology for hyperbolic systems with stiff relaxation was carried out recently in [22]. The BGK penalization method has also been extended to the Fokker–Planck–Laudau equation [23], the quantum Boltzmann equation [24], and the quantum Fokker–Planck–Landau equation [25].

In this article, we generalize the BGK-penalization idea of Filbet–Jin to the multispecies Boltzmann equation. Several new difficulties arise here. First, there are several possible choices of the local Maxwellian, and one has to determine the one that suits our needs. We found that a suitable choice is the local Maxwellian that depends on the "mean" velocity and mean temperature. Second, to justify various AP properties, one needs to prove that the velocities and temperatures of different species equilibrate, a property one does not encounter for the single species Boltzmann equation. We justify this property for the proposed scheme, in the relaxed-AP sense. Finally, we demonstrate that this method can also be used for gas mixtures with disparate masses, which arises in ion–electron evolution problem in plasma [26–29].

This article is organized as follows. We describe the Boltzmann equation for the multispecies system and one of its related BGK models in Section II, including their theoretical properties. In Section III, we give details of the numerical scheme. This is followed by Section IV where we prove various AP properties of the scheme. In Section V, we discuss the disparate masses system. We show several numerical examples in Section VI.

II. THE MULTISPECIES MODELS

A. The Multispecies Boltzmann Equation

The Boltzmann equation describes the evolution of the density distribution of rarefied gases. We use $f_i(t, x, v)$ to represent the distribution function of the ith species at time t on the phase space (x, v), and $f = (f_1, f_2, \cdots, f_N)^T$. The Boltzmann equation for the multispecies system is given by [30]:

$$\partial_t f_i + v \cdot \nabla_x f_i = Q_i(f, f), \quad t \geq 0, (x, v) \in \mathbb{R}^d \times \mathbb{R}^d, \tag{1}$$

with

$$Q_i(f,f) = \sum_{k=1}^{N} Q_{ik}(f,f), \tag{2a}$$

$$Q_{ik}(f,f)(v) = \int_{S_+^{d-1}} \int_{\mathbb{R}^d} \left(f_i' f_{k*}' - f_i f_{k*}\right) B_{ik}(|v - v_*|, \Omega) dv_* d\Omega, \tag{2b}$$

where x is the position of the particle, B_{ik} is the collision kernel, and $B_{ik} = B_{ki}$, (thus $Q_{ik} = Q_{ki}$); v, v_* are precollisional velocities; v' and v_*' are postcollisional velocities; $f_i' = f_i(t,x,v')$ and $f_{k*}' = f_k(t,x,v_*')$; Ω is a unit vector, and S_+^{d-1} is the semisphere defined by $g \cdot \Omega \geq 0$, where g is relative velocity

$$g = v - v_*.$$

There are many variations for the collision kernel B_{ik}. One of the simple cases is the Maxwell molecule when $B_{ik} = B_{ik}\left(\frac{g\cdot\Omega}{|g|}\right)$. The postcollisional velocities v' and v_*' satisfy:

$$v' = v - \frac{2\mu_{ik}}{m_i}(g \cdot \Omega)\Omega, \tag{3a}$$

$$v_*' = v_* + \frac{2\mu_{ik}}{m_k}(g \cdot \Omega)\Omega, \tag{3b}$$

with $\mu_{ik} = \frac{m_i m_k}{m_i + m_k}$ being the reduced mass and m_i and m_k being the mass for species i and k, respectively. This deduction is based on momentum and energy conservations:

$$m_i v + m_k v_* = m_i v' + m_k v_*',$$
$$m_i |v|^2 + m_k |v_*|^2 = m_i |v'|^2 + m_k |v_*'|^2.$$

B. Properties of the Multispecies Boltzmann Equation

In d-dimensional space, we define the macroscopic quantities for species i: n_i is the number density; ρ_i is the mass density; u_i is the average velocity; E_i is the total energy; e_i is the specific internal energy; T_i is the temperature; S_i is the stress tensor; and q_i is the heat flux vector, given by:

$$n_i = \int f_i dv, \quad \rho_i = m_i n_i,$$

$$\rho_i u_i = m_i \int v f_i dv,$$

$$E_i = \frac{1}{2}\rho_i u_i^2 + n_i e_i = \frac{1}{2} m_i \int |v|^2 f_i dv,$$

$$e_i = \frac{d}{2} T_i = \frac{m_i}{2n_i} \int f_i |v - u_i|^2 dv,$$

$$S_i = \int (v - u_i) \otimes (v - u_i) f_i dv,$$

$$q_i = \frac{1}{2} m_i \int (v - u_i) |v - u_i|^2 f_i dv. \tag{4}$$

We also have global quantities for the mixture: the total mass density ρ, the number density n, the mean velocity $\bar{u}$, the total energy E, the internal energy $n\bar{e}$, and the mean temperature $\bar{T} = \frac{2\bar{e}}{d}$ are defined by:

$$\rho = \sum_i \rho_i, \quad n = \sum_i n_i, \tag{5a}$$

$$\rho\bar{u} = \sum_i \rho_i u_i, \tag{5b}$$

$$E = n\bar{e} + \frac{1}{2}\rho|\bar{u}|^2 = \frac{d}{2}n\bar{T} + \frac{\rho}{2}|\bar{u}|^2 = \sum_i E_i. \tag{5c}$$

Conservations. In the gas mixture system, for each species, the mass is conserved but not the momentum and energy. This means that the first moment of the collision term is zero, but the second and the third are not. They are obtained by multiplying the collision term with $\phi = m_i\left(1, v, \frac{1}{2}|v|^2\right)^T$ and then integrating with respect to v. Usually, explicit expressions for these moments cannot be obtained, but for some special case, for example, the Maxwell molecule, explicit expression is available:

$$\begin{aligned}
\langle m_i Q_i\rangle &= \int m_i Q_i(f)dv = 0,\\
\langle m_i v Q_i\rangle &= \int m_i v Q_i(f)dv = \sum_{k=1}^{n} 2\mu_{ik}\chi_{ik}n_i n_k[u_k - u_i],\\
\left\langle \frac{1}{2}m_i v^2 Q_i\right\rangle &= \int \frac{m_i}{2}|v|^2 Q_i(f)dv\\
&= \sum_{k=1}^{n} 2m_i\chi_{ik}n_i n_k\left[\left(\frac{\mu_{ik}}{m_i}\right)^2\left(|u_k - u_i|^2 + 2\frac{e_k}{m_k} + 2\frac{e_i}{m_i}\right)\right.\\
&\quad \left. + \frac{\mu_{ik}}{m_i}\left((u_k - u_i)\cdot u_i - 2\frac{e_i}{m_i}\right)\right],
\end{aligned} \tag{6}$$

where $\chi_{ik} = \int(\cos\theta)^2 B_{ik}(\theta)d\theta$, with $\theta = \arccos(\frac{g\cdot\Omega}{|g|})$. One can check [31] for power law molecules.

Based on these formulas, when taking moments of the Boltzmann equation, one obtains the corresponding evolution of the macroscopic quantities. Taking the 1D Maxwell molecule, for example,

$$\begin{aligned}
&\partial_t\rho_i + \partial_x(\rho_i u_i) = \langle m_i Q_i\rangle = 0, \qquad \text{or} \qquad \partial_t n_i + \partial_x(n_i u_i) = 0,\\
&\partial_t(\rho_i u_i) + \partial_x(S_i + \rho_i u_i^2) = \frac{1}{\varepsilon}\langle m_i v Q_i\rangle = \frac{1}{\varepsilon}\sum_k 2B_{ik}n_i n_k\mu_{ik}[u_k - u_i],\\
&\partial_t E_i + \partial_x(E_i u_i + S_i u_i + q_i) = \frac{1}{\varepsilon}\left\langle \frac{1}{2}m_i|v|^2 Q_i\right\rangle = \frac{1}{\varepsilon}\sum_k 2B_{ik}n_i n_k\left(\frac{\mu_{ik}^2}{m_i m_k}\right)(a+b),
\end{aligned} \tag{7}$$

where $a = (m_k u_k + m_i u_i) \cdot (u_k - u_i)$ and $b = 2(e_k - e_i)$. However, the total momentum and total energy are still conserved. By summing up the momentum and energy equations for all species, one obtains:

$$\partial_t(\rho\bar{u}) + \partial_x\left(\sum_i S_i + \sum_i \rho_i u_i^2\right) = \frac{1}{\varepsilon}\sum_i \langle m_i v_i Q_i\rangle = 0,$$
$$\partial_t E + \partial_x\left(\sum_i E_i u_i + \sum_i S_i u_i + \sum_i q_i\right) = \frac{1}{\varepsilon}\sum_i \left\langle \frac{1}{2} m_i v_i^2 Q_i \right\rangle = 0. \tag{8}$$

These hold for all kinds of cross-sections.

The Local Maxwellian. The local equilibrium is reached when the gaining part and losing part of collision terms balance out, namely $Q_i(f) = 0$ for each i. It is given by [32]:

$$f_i = \overline{M}_i = n_i\left(\frac{m_i}{2\pi\bar{T}}\right)^{d/2} e^{-\frac{m_i|v-\bar{u}|^2}{2\bar{T}}}, \tag{9}$$

where $\bar{T}$ is the mean temperature and $\bar{u}$ is mean velocity defined in (2.5). We call this Maxwellian the "unified Maxwellian," because the velocity $\bar{u}$ and temperature $\bar{T}$ are given by those for the entire system instead of those for each single species.

The Euler Limit. Expanding f_i around the unified Maxwellian (9), the standard Chapman-Enskog expansion shows that at the local equilibrium, the collision term vanishes, and the system yields its Euler limit [32]:

$$\partial_t \rho_i + \nabla\cdot(\rho_i\bar{u}) = 0,$$
$$\partial_t(\rho\bar{u}) + \nabla\cdot(\rho\bar{u}\otimes\bar{u} + n\bar{T}\mathbb{I}) = 0,$$
$$\partial_t E + \nabla\cdot((E + n\bar{T})\bar{u}) = 0. \tag{10}$$

Here $\mathbb{I}$ is the identity matrix. Note that in the equation for ρ_i, we have $\bar{u}$ instead of u_i as in (7). This is because when $\varepsilon \to 0$, $u_i \to \bar{u}$, and $T_i \to \bar{T}$ for all i.

C. A BGK Model

The BGK operator is a classical approximation for the Boltzmann collision operator. There are several BGK models, but most of them either suffer from the loss of positivity [33] or fail to satisfy the indifferentiability principle [34]. The positivity guarantees that the distribution function is always positive, and indifferentiability requires that when different species share the same mass, equations of the system should be consistent with the single species Boltzmann equation. We choose the BGK model proposed by Andries et al. [32], the one that guarantees both of these two properties.

The model reads:

$$\partial_t f_i + v\cdot\nabla_x f_i = \frac{\nu_i}{\varepsilon}(\widetilde{M}_i - f_i), \tag{11}$$

with ν_i being collision frequency and $\widetilde{M}_i$ being a Maxwellian:

$$\nu_i = \sum_k n_k \chi_{ik},$$
$$\widetilde{M}_i = n_i \left(\frac{m_i}{2\pi \widetilde{T}_i}\right)^{d/2} e^{-\frac{m_i|v-\widetilde{u}_i|^2}{2\widetilde{T}_i}}. \tag{12}$$

The way $\widetilde{M}$ is defined is to capture the moments of the collision Q, that is, $\nu_i(\widetilde{M}_i - f_i)$ shares the same first five moments as Q_i. For the Maxwell molecule, explicit expressions are computed from (6):

$$\nu_i \rho_i \widetilde{u}_i - \nu_i \rho_i u_i = \langle m_i v Q_i \rangle = \sum_{k=1}^{n} 2\mu_{ik}\chi_{ik} n_i n_k [u_k - u_i], \tag{13a}$$

$$\begin{aligned} \nu_i \widetilde{E}_i - \nu_i E_i &= \left\langle \frac{1}{2} m_i v^2 Q_i \right\rangle \\ &= \sum_{k=1}^{n} 2m_i \chi_{ik} n_i n_k \left[\left(\frac{\mu_{ik}}{m_i}\right)^2 \left(|u_k - u_i|^2 + 2\frac{e_k}{m_k} + 2\frac{e_i}{m_i} \right) \right. \\ &\quad \left. + \frac{\mu_{ik}}{m_i} \left((u_k - u_i) \cdot u_i - 2\frac{e_i}{m_i} \right) \right], \end{aligned} \tag{13b}$$

and $\widetilde{T}_i = (2\widetilde{E}_i - \rho_i \widetilde{u}_i^2)/(n_i d)$. Note that the right hand side of Eq. (13a) is just a linear operator of macroscopic velocities. Also, when u is known, the right hand side of (13b) is linear on e. For later reference, we define a matrix $\mathbb{L}$ by:

$$(\mathbb{L})_{ij} = \begin{cases} 2\mu_{ij}\chi_{ij} n_i n_j, & i \neq j, \\ -2\sum_k \mu_{ik}\chi_{ik} n_i n_k, & i = j. \end{cases} \tag{14}$$

Apparently, $\mathbb{L}$ is a symmetric matrix with each row summing up to 0, and all nondiagonal entries are positive. As $\mathbb{L}$ is a symmetric weakly diagonally dominant matrix, it is seminegative definite, that is, all its eigenvalues are nonpositive. Under this definition, Eq. (13a) turns out to be $\nu_i \rho_i \widetilde{u}_i - \nu_i \rho_i u_i = \mathbb{L}u$. For later convenience, we denote $\lambda(\mathbb{M})$ the spectral radius of matrix $\mathbb{M}$:

$$\lambda(\mathbb{M}) = \sup_i (|\lambda_i(\mathbb{M})|), \tag{15}$$

where $\lambda_i(\mathbb{M})$ are eigenvalues of $\mathbb{M}$.

We also mention another type of Maxwellian, which is defined by macroscopic quantities u_i and T_i for each species. We call it the "species Maxwellian":

$$M_i = n_i \left(\frac{m_i}{2\pi T_i}\right)^{d/2} e^{-\frac{m_i|v-u_i|^2}{2T_i}}. \tag{16}$$

Remark 1. *$M_i - f_i$ cannot be used as a BGK operator. In the multispecies system, one has to introduce some mechanism into the collision term that captures the interactions between species. $M_i - f_i$ gives no communication between the species, so it cannot be used to express the multispecies collision.*

III. AN AP SCHEME FOR THE MULTISPECIES BOLTZMANN EQUATION

In this chapter, we derive our AP scheme for the multispecies Boltzmann equation. Our idea is based on the BGK-penalization method proposed by Filbet and Jin [12].

A. The time discretization

Here, we adopt the same strategy and write our scheme as:

$$\frac{f_i^{l+1} - f_i^l}{\Delta t} + v \cdot \nabla_x f_i^l = \frac{Q_i(f^l) - P_i(f^l)}{\varepsilon} + \frac{P_i(f^{l+1})}{\varepsilon}. \tag{17}$$

The superscript l stands for the time step. Later, we will use $Q_i^l \triangleq Q_i(f^l)$, $P_i^l \triangleq P_i(f^l)$ for convenience. P_i is chosen to be the BGK operator:

$$P_i = \beta(\overline{M}_i - f_i), \tag{18}$$

where β is a positive constant chosen for stability and positivity, see Section III-D. A simple algebraic manipulation on (3.1) gives:

$$f_i^{l+1} = \frac{\varepsilon f_i^l + \Delta t\left(Q_i^l - \beta^l\left(\overline{M}_i^l - f_i^l\right)\right) - \varepsilon \Delta t\, v \cdot \nabla_x f_i^l + \beta^{l+1}\Delta t \overline{M}_i^{l+1}}{\varepsilon + \beta^{l+1}\Delta t}. \tag{19}$$

The computation of the collision term Q_i and the flux term $v \cdot \nabla_x f$ is relatively classical and will be given later; $\overline{M}_i$ is defined in (9); and the choice of β is also going to be presented later.

B. The Computation of $\overline{M}^{l+1}$

Taking moments of (17), one gets:

$$n_i^{l+1} = n_i^l - \Delta t \int v \cdot \nabla_x f_i^l \, dv,$$

$$(\rho\bar{u})^{l+1} = (\rho\bar{u})^l - \Delta t \sum_i m_i \int v \otimes v \nabla_x f_i^l \, dv,$$

$$E^{l+1} = E^l - \Delta t \sum_i \int \frac{m_i}{2} |v|^2 v \cdot \nabla_x f_i^l \, dv,$$

and by the definition of $\bar{T}$ in (5c),

$$\bar{T}^{l+1} = \frac{2E^{l+1} - (\rho\bar{u}^2)^{l+1}}{dn^{l+1}}.$$

The discretization of the flux term will be discussed in Section III-E.

C. The Collision Term Q

We use the spectral method introduced in [35] to compute the collision term Q_i. Use a ball $B(0, S)$ to represent the domain of the compactly supported distribution f. Then, we periodize

f on $v \in [-L, L]^d$ with $L \geq (3+\sqrt{2})S$. L is chosen much larger than S to avoid nonphysical collision at different periods of the periodized f. Define the Fourier transform as:

$$\hat{f}(x;p) = \int f(x;v)e^{-ip\cdot v}\,dv,$$
$$f(x;v) = \frac{1}{(2L)^d}\sum_p \hat{f}(x;p)e^{ik\cdot v}. \tag{20}$$

Plugging into the collision term (2b):

$$Q_{ik} = \iint B_{ik}\left[f_i' f_{k*}' - f_i f_{k*}\right]dv_* d\Omega \equiv Q_{ik}^+ - f_i Q_{ik}^-,$$

where we define the gaining part and losing part as:

$$Q_{ik}^+ = \iint B_{ik}\left(f_i' f_{k*}'\right)dv_* d\Omega, \quad f_i Q_{ik}^- = \iint B_{ik}(f_i f_{k*})dv_* d\Omega = f_i \iint B_{ik} f_{k*} dv_* d\Omega.$$

Using the Fourier transform (20), one gets:

$$Q_{ik}^+ = \iint \frac{B_{ik}}{(2L)^{2d}}\left[\sum_p\sum_q \hat{f}_i(x;p)e^{ip\cdot v'}\hat{f}_k(x;q)e^{iq\cdot v_*'}\right]dv_* d\Omega.$$

For easier computation, one can rewrite Eqs. (3) to:

$$v' = v - \frac{\mu_{ik}}{m_i}(g - |g|\omega), \quad v_*' = v_* + \frac{\mu_{ik}}{m_k}(g - |g|\omega) = v - g + \frac{\mu_{ik}}{m_k}(g - |g|\omega).$$

Note the domain for ω is the entire unit sphere S^{d-1} instead of the semisphere for Ω. Then:

$$\begin{aligned} Q_{ik}^+ &= \frac{1}{(2L)^{2d}}\sum_{p,q}\hat{f}_i^p\hat{f}_k^q\iint B_{ik}e^{i(p\cdot v'+q\cdot v_*')}dv_* d\omega \\ &= \frac{1}{(2L)^{2d}}\sum_{p,q}\hat{f}_i^p\hat{f}_k^q e^{i(p+q)\cdot v}\iint B_{ik}e^{i\lambda\cdot g + i|g|\gamma\cdot\omega}dv_* d\omega, \end{aligned}$$

where $\lambda = \frac{-m_k}{m_i+m_k}p + \frac{-m_k}{m_i+m_k}q$ and $\gamma = \frac{m_k}{m_i+m_k}p - \frac{m_i}{m_i+m_k}q$. Given a specific B_{ik} one can analytically compute the integration above. The expression, however, can be very tedious, even in one-dimensional (1D) space, especially when B_{ik} depends on $|g|$. Note that the integration domain for g is not symmetric. But for the 1D Maxwell molecule, B_{ik} is a constant and can be pulled out of the integral, making the computation much easier. We show examples for the 1D Maxwell molecule and leave other situations for further discussions. In this case,

$$v' = v - \frac{2m_k}{m_i+m_k}(v - v_*) = \frac{m_i - m_k}{m_i+m_k}v + \frac{2m_k}{m_i+m_k}v_*,$$
$$v_*' = v + \frac{m_i - m_k}{m_i+m_k}(v - v_*) = \frac{2m_i}{m_i+m_k}v - \frac{m_i - m_k}{m_i+m_k}v_*.$$

Plugging in Q_{ik}^+, one gets:

$$Q_{ik}^+ = \frac{B_{ik}}{(2L)^2}\sum_{p,q}\hat{f}_i^p\hat{f}_k^q e^{i\left(\frac{m_i-m_k}{m_i+m_k}p+\frac{2m_i}{m_i+m_k}q\right)v}\int e^{i\left(\frac{2m_k}{m_i+m_k}p-\frac{m_i-m_k}{m_i+m_k}q\right)v_*}dv_*.$$

One can also write Q_{ik}^+ as a summation of its Fourier modes $Q_{ik}^+(v) = \frac{1}{(2L)^2}\sum_l \hat{Q}_{ik}^{l+}e^{ilv}$ where

$$\begin{aligned}\hat{Q}_{ik}^{l+} &= \int Q_{ik}^+ e^{-ilv}dv\\ &= \frac{B_{ik}}{(2L)^2}\sum_{p,q}\hat{f}_i^p\hat{f}_k^q\int e^{i\left(\frac{m_i-m_k}{m_i+m_k}p+\frac{2m_i}{m_i+m_k}q-l\right)v}dv\int e^{i\left(\frac{2m_k}{m_i+m_k}p-\frac{m_i-m_k}{m_i+m_k}q\right)v_*}dv_*\\ &= B_{ik}\sum_{p,q}\hat{f}_i^p\hat{f}_k^q\,\mathrm{sinc}(a)\,\mathrm{sinc}(b),\end{aligned}$$

where $a = \left(\frac{m_i-m_k}{m_i+m_k}p+\frac{2m_i}{m_i+m_k}q-l\right)L$ and $b = \left(\frac{2m_k}{m_i+m_k}p-\frac{m_i-m_k}{m_i+m_k}q\right)L$. The FFT and the inverse FFT are used to speed up the computation.

The computation for $f_iQ_{ik}^-$ is much simpler in this special case: $f_iQ_{ik}^- = f_i\int B_{ik}f_k dv_k = f_in_kB_{ik}$.

After getting all Q_{ik}, $Q_i = \sum_k Q_{ik}$.

D. The Choice of the Free Parameter β

β should be chosen as the maximum value of the Frechet derivative $\nabla Q_i(f)$ [12]. Numerically, to guarantee positivity, one can split the collision Q into the gaining part and the losing part $Q_i = Q_i^+ - f_iQ_i^-$ by $Q_i^+ = \sum_k Q_{ik}^+$ and $f_iQ_i^- = f_i\sum_k Q_{ik}^-$. Plug back in the scheme (19), one can rearrange the scheme:

$$f_i^{l+1} = \frac{\varepsilon\left(f_i^l - \Delta t\, v\cdot\nabla_x f_i^l\right) + \Delta t\, Q_i^+(f^l) + \left[\left(\beta^l - Q_i^-(f^l)\right)f_i^l + \beta^{l+1}\overline{M}_i^{l+1} - \beta^l\overline{M}_i^l\right]\Delta t}{\varepsilon + \beta^{l+1}\Delta t}. \tag{21}$$

To obtain positivity, it is sufficient to require the followings for all i [20]:

$$\beta^l > Q_i^-(f^l),$$
$$\beta^l\overline{M}_i^l > \beta^{l-1}\overline{M}_i^{l-1}.$$

E. The Flux Term $v\cdot\nabla_x f_i$

Here, we give the numerical flux in 1D. Use $v\partial_x f_{i,j}$ to denote the flux term for species i at the grid point x_j. A shock-capturing finite volume method we use is [36]:

$$v\partial_x f_{i,j} = \nu(f_{i,j_1} - f_{i,j_1-1}) - \frac{1}{2}\nu(\mathrm{sgn}(\nu)-\nu)(h\sigma_{i,j_1} - h\sigma_{i,j_1-1}), \tag{22}$$

where $\nu = \frac{v}{h}$, h is the mesh size. j_1 is chosen to be j for $v > 0$ and $j+1$ for $v < 0$. $\sigma_{i,j} = \frac{f_{i,j+1}-f_{i,j}}{h}\phi_{i,j}$ where $\phi_{i,j}$ is the slope limiter. For the van Leer limiter, it takes value as $\phi(\theta) = \frac{\theta+|\theta|}{\theta+1}$ and $\theta_{i,j} = \frac{f_{i,j}-f_{i,j-1}}{f_{i,j+1}-f_{i,j}}$ reflects the smoothness around grid point x_j.

The discretization for the flux term in higher dimension uses the dimension-by-dimension approach.

IV. THE AP PROPERTY OF THE TIME DISCRETIZATION

The time discrete scheme (17) is written as:

$$\frac{f_i^{l+1}-f_i^l}{\Delta t}+v\cdot\nabla_x f_i^l=\frac{Q_i^l-\beta\big(\overline{M}_i^l-f_i^l\big)}{\varepsilon}+\frac{\beta\big(\overline{M}_i^{l+1}-f_i^{l+1}\big)}{\varepsilon}. \tag{23}$$

We will show below that this method is weakly AP for the Maxwell molecule, and relaxed-AP for the BGK model given in Section II-C. Later, we always assume that $\Delta t \gg \varepsilon$. Besides the definition for the linear operator $\mathbb{L}$ in (14) and $\lambda(\mathbb{M})$ in (15), we also define:

$$\delta u_i^l=u_i^l-\bar{u}^l,\quad \delta T_i^l=T_i^l-\bar{T}^l, \tag{24}$$

and

$$\mathbb{D}=\begin{bmatrix}\rho_1 & 0 & \dots & 0\\ 0 & \rho_2 & \ddots & \vdots\\ \vdots & \ddots & \ddots & \vdots\\ 0 & \dots & \dots & \rho_N\end{bmatrix}. \tag{25}$$

A. Weakly AP

Lemma 4.1. *For the Maxwell molecule, if $\delta u_i^l = O(\varepsilon)$ and $\delta T_i^l = O(\varepsilon)$ for $\forall i$, then $\delta u_i^{l+1} = O(\varepsilon)$ and $\delta T_i^{l+1} = O(\varepsilon)$.*

Proof. Rewrite scheme (23) as:

$$f_i^{l+1}-\overline{M}_i^{l+1}=\frac{\varepsilon\big(-\overline{M}_i^{l+1}+\overline{M}_i^l\big)-\varepsilon\Delta t\, v\cdot\nabla_x f_i^l}{\varepsilon+\beta\Delta t}+\frac{\Delta t\, Q_i^l}{\varepsilon+\beta\Delta t}-\big(\overline{M}_i^l-f_i^l\big). \tag{26}$$

Take the first moment on both sides. On the left hand side, one gets $(\rho_i u_i)^{l+1}-(\rho_i\bar{u})^{l+1}$, whereas on the right hand side, the first term is $O(\varepsilon)$. The second term gives:

$$\begin{aligned}\frac{\Delta t}{\varepsilon+\beta\Delta t}\langle m_i v Q_i^l\rangle &= \frac{\Delta t}{\varepsilon+\beta\Delta t}\sum_k 2\chi_{ik}\mu_{ik}n_i n_k\big[u_k^l-u_i^l\big]\\ &= \frac{\Delta t}{\varepsilon+\beta\Delta t}\sum_k 2\chi_{ik}\mu_{ik}n_i n_k\big(\delta u_k^l-\delta u_i^l\big)=O(\varepsilon).\end{aligned} \tag{27}$$

The third term gives:

$$\Big\langle m_i v\big(\overline{M}_i^l-f_i^l\big)\Big\rangle=\rho_i\big(\bar{u}^l-u_i^l\big)=O(\varepsilon).$$

So the entire right hand side is of $O(\varepsilon)$, thus the term on the left hand side, $(\rho_i u_i)^{l+1}-(\rho_i\bar{u})^{l+1}=O(\varepsilon)$, that is, $\delta u_i^{l+1}=O(\varepsilon)$. Similar analysis can be carried out for T. ∎

Remark 2. *In the proof, we used that the collision kernel is for the Maxwell molecule in (27). The proof can be extended to other collision kernels as long as one can show the moments of Q is of $O(\varepsilon)$ whenever $\delta u = O(\varepsilon)$.*

Theorem 4.1. *The method is weakly AP; namely, if $\overline{M}_i^l - f_i^l = O(\varepsilon)$, then $\overline{M}_i^{l+1} - f_i^{l+1} = O(\varepsilon)$.*

Proof. As $\overline{M}_i^l - f_i^l = O(\varepsilon)$, both $P_i(f^l)$ and $Q_i(f^l)$ are of $O(\varepsilon)$. Plugging back into the scheme (26), one gets $f_i^{l+1} - \overline{M}_i^{l+1} = O(\varepsilon)$. ∎

B. Relaxed-AP

Lemma 4.2. *For the Maxwell molecules, when $\Delta t \ll 1$, in the limit of $\varepsilon \to 0$, there $\exists L$, such that $\forall l > L$, $\delta u^l = O(\varepsilon)$, given big enough β.*

Proof. We prove the result for the 1D case. The proof for higher dimension can be carried out similarly. The proof follows that of [12]. One can take moments of numerical scheme (23):

$$\frac{(\rho u)^{l+1} - (\rho u)^l}{\Delta t} + \partial_x \int v^2 m f^l dv = \frac{1}{\varepsilon}(\mathbb{L}^l u^l + \beta^l \mathbb{D}^l \delta u^l - \beta^{l+1}\mathbb{D}^{l+1}\delta u^{l+1}),$$

$$\Rightarrow \quad (\varepsilon + \beta^{l+1}\Delta t)\mathbb{D}^{l+1}\delta u^{l+1}$$

$$= ((\varepsilon + \beta^l \Delta t)\mathbb{D}^l + \Delta t \mathbb{L}^l)\delta u^l + \varepsilon((\rho\bar{u})^l - (\rho\bar{u})^{l+1}) - \varepsilon\Delta t\partial_x \int v^2 m f^l dv,$$

$$\Rightarrow \quad (\varepsilon + \beta^{l+1}\Delta t)(\mathbb{D}^l + O(\Delta t))\delta u^{l+1} = [(\varepsilon + \beta^l \Delta t)\mathbb{D}^l + \Delta t \mathbb{L}^l]\delta u^l + O(\varepsilon),$$

where $\mathbb{L}^l \bar{u} = 0$ and $\mathbb{D}^{l+1} = \mathbb{D}^l + O(\Delta t)$ were used.

After some simple algebra, one can rewrite the previous equation as:

$$\delta u^{l+1} = \left[\frac{\beta^l}{\beta^{l+1}}\mathbb{I} + \frac{1}{\beta^{l+1}}(\mathbb{D}^l)^{-1}\mathbb{L}^l + O(\Delta t)\right]\delta u^l + O(\varepsilon).$$

Define $\mathbb{A}_u$ as:

$$\mathbb{A}_u = \left[\frac{\beta^l}{\beta^{l+1}}\mathbb{I} + \frac{1}{\beta^{l+1}}(\mathbb{D}^l)^{-1}\mathbb{L}^l + O(\Delta t)\right]. \tag{28}$$

As the eigenvalues for $\mathbb{L}$ are nonpositive, if one chooses $\beta^{l+1} + \beta^l > \lambda((\mathbb{D}^l)^{-1}\mathbb{L}^l)$, given small enough Δt, $|\lambda(\mathbb{A}_u)| < 1$, thus in the limit of $\varepsilon \to 1$, δu would decrease to $O(\varepsilon)$, and we get our conclusion. ∎

The same analysis can be carried out for T. We call this property proved above "macro-AP."

Remark 3. *The proof earlier is also valid for the BGK model in Section II-C. It can also be extended to other kinds of collision kernel, but the corresponding $\mathbb{L}$ may not be linear on u, and the requirement on β may not have an explicit expression. In that case, one needs to define $\lambda(\mathbb{L})$ as the spectrum of the nonlinear operator $\mathbb{L}$.*

Theorem 4.2. *If the problem is macro-AP, then, $\exists L$ such that $\forall l > L$, $M_i^l - \overline{M}_i^l = O(\varepsilon)$, and $\widetilde{M}_i^l - \overline{M}_i^l = O(\varepsilon)$.*

Proof. It is a straightforward conclusion from the lemma earlier, and from the definition for $\widetilde{M}$ in (12). ∎

Remark 4. *Up to now, we have shown that M_i approaches to $\overline{M}_i$ for the Boltzmann collision operator with the Maxwell molecule collision kernel. Rearranging scheme (23), one gets:*

$$f^{l+1} - \overline{M}^{l+1} = \frac{(\varepsilon + \beta\Delta t)(f^l - \overline{M}^l) + \Delta t\, Q^l}{\varepsilon + \beta\Delta t} + \frac{\varepsilon(\overline{M}^l - \overline{M}^{l+1}) - \varepsilon\Delta t\, v \cdot \nabla_x f^l}{\varepsilon + \beta\Delta t}. \tag{29}$$

The second term on the right is of $O(\varepsilon)$. So, one can get relaxed-AP only if it can be shown that Q and $f - \overline{M}$ have opposite signs. We can prove this for limited form of Q, say the BGK operator introduced in Section II-C. Later in Section VI, we will show that numerically the scheme is relaxed-AP for the general Boltzmann collision defined in (2).

Theorem 4.3. *The scheme is relaxed-AP for the BGK operator $Q = \nu(\widetilde{M} - f)$ defined in Section II-C.*

Proof. Plug in the definition for Q, (29) writes:

$$\begin{aligned} f^{l+1} - \overline{M}^{l+1} &= \frac{\varepsilon + \beta\Delta t - \nu\Delta t}{\varepsilon + \beta\Delta t}(f^l - \overline{M}^l) + \frac{\nu\Delta t(\widetilde{M}^l - \overline{M}^l)}{\varepsilon + \beta\Delta t} + O(\varepsilon) \\ &= \frac{\varepsilon + \beta\Delta t - \nu\Delta t}{\varepsilon + \beta\Delta t}(f^l - \overline{M}^l) + O(\varepsilon) \end{aligned}$$

The second equality comes from Theorem 4.2 and Remark 3. Define:

$$\alpha = \frac{\varepsilon + \beta\Delta t - \nu\Delta t}{\varepsilon + \beta\Delta t}, \tag{30}$$

and we call it the convergent rate to the unified Maxwellian $\overline{M}$. In the limit of $\varepsilon \to 0$, if one has $\beta > \frac{\nu}{2}$, then $|\alpha| < 1$, thus $|f - \overline{M}|$ keeps diminishing until reaching to $O(\varepsilon)$, and we get the relaxed-AP. ∎

V. DISPARATE MASSES

This section is for the system of gas mixture with disparate masses in the space homogeneous case. The mathematical problem was first pointed out by Grad [26] and has attracted great interests since then. The fundamental example is plasma, for which, the basic derivation can be found in [27, 28]. For these systems, it is the different time scalings for different species to reach to the equilibria that makes the problem difficult. Generally speaking, the light species should be able to get to the equilibrium faster, that is to say there is a time period when the light species is in hydrodynamic regime while the heavy species is, on the other hand, in kinetic regime. Analyses of the scalings of the collision operators have been done based on both postulate physical consideration [37, 38] and formal derivation [39, 40].

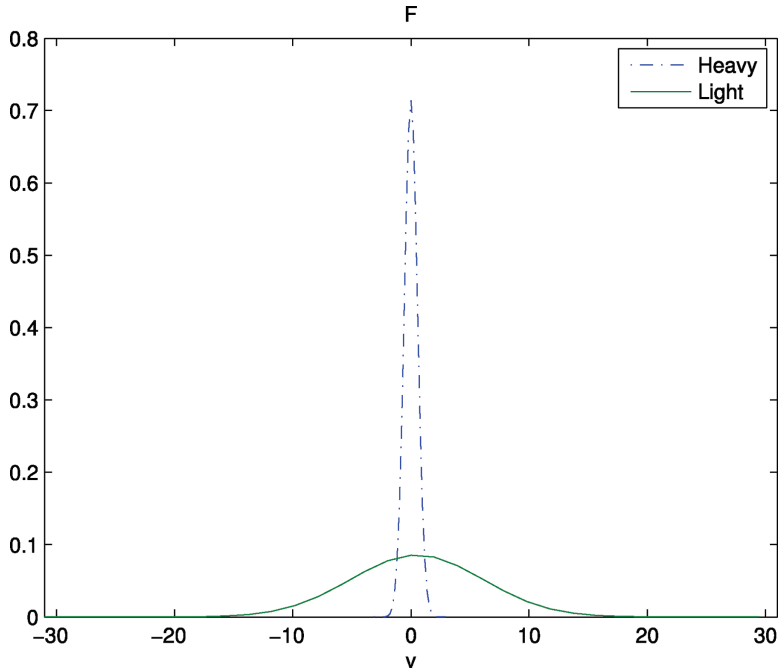

FIG. 1. Distribution for heavy species is much narrower than that of the light species. [Color figure can be viewed in the online issue, which is available at wileyonlinelibrary.com.]

A. Theoretical Rescaling Analysis

In homogeneous space, the disparate masses system should be written as:

$$\begin{cases} \partial_t f_{\mathrm{H}} = Q_{\mathrm{H}} = Q_{\mathrm{HH}} + Q_{\mathrm{HL}} = \int B_{\mathrm{HH}}\left(f'_{\mathrm{H}} f'_{\mathrm{H}*} - f_{\mathrm{H}} f_{H*}\right) dv_* + \int B_{\mathrm{HL}}\left(f'_{\mathrm{H}} f'_{\mathrm{L}*} - f_{\mathrm{H}} f_{\mathrm{L}*}\right) dv_*, \\ \partial_t f_{\mathrm{L}} = Q_{\mathrm{L}} = Q_{\mathrm{LL}} + Q_{\mathrm{LH}} = \int B_{\mathrm{LL}}\left(f'_{\mathrm{L}} f'_{\mathrm{L}*} - f_{\mathrm{L}} f_{\mathrm{L}*}\right) dv_* + \int B_{\mathrm{LH}}\left(f'_{\mathrm{H}*} f'_{\mathrm{L}} - f_{\mathrm{H}*} f_{\mathrm{L}}\right) dv_*. \end{cases} \tag{31}$$

Now, the small parameter that makes the collision term stiff is the ratio of mass $\varepsilon = \sqrt{m_{\mathrm{L}}/m_{\mathrm{H}}}$ where the subindices H and L stand for heavy and light, respectively. While assuming that the two species have densities and temperatures of the same order of magnitude, one could obtain that f_{H} is much narrower than f_{L} as shown in Fig. 1. To analyze the magnitude of the collision terms, we define $\tilde{f}_{\mathrm{H}}(v) = f_{\mathrm{H}}(\varepsilon v)$ to stretch f_{H} to a function that has comparable variance as f_{L}. As derived in [39, 40], the scaling ratio of the two collision terms is $Q_{\mathrm{H}}/Q_{\mathrm{L}} = O(\varepsilon)$, which means that the collision Q_{L} has stronger effect and that the light species gets to the hydrodynamical regime much faster. For convenience, we write both Q_{H} and Q_{L} as $O(1)$ term and put ε in front of Q_{H} to represent its magnitude. The system turns out to be:

$$\begin{cases} \partial_t f_{\mathrm{H}} = \varepsilon Q_{\mathrm{H}}, \\ \partial_t f_{\mathrm{L}} = Q_{\mathrm{L}}. \end{cases} \tag{32}$$

One can also rescale the time by τ and obtain:

$$\begin{cases} \partial_t f_{\mathrm{H}} = \dfrac{\varepsilon}{\tau} Q_{\mathrm{H}}, \\ \partial_t f_{\mathrm{L}} = \dfrac{1}{\tau} Q_{\mathrm{L}}. \end{cases} \tag{33}$$

When $\tau = O(\varepsilon)$, the light species is in hydrodynamic regime, but the heavy one is still in kinetic regime; and when $\tau = O(\varepsilon^2)$, both species should be close to the equilibria.

Remark 5. *The inhomogeneous problem gets even harder to analyze, especially when the different species have different spatial rescaling coefficients. But numerically it makes very little difference: one simply needs to add the flux term $v \cdot \nabla_x f$ to the homogeneous scheme.*

B. The Numerical Scheme

The scheme we adopt for (32) is:

$$\frac{f_{\mathrm{H}}^{l+1} - f_{\mathrm{H}}^{l}}{\Delta t} = \frac{\varepsilon}{\tau}\big(Q_{\mathrm{H}}^{l} - \beta\big(M_{\mathrm{H}}^{l} - f_{\mathrm{H}}^{l}\big)\big) + \frac{\beta\varepsilon}{\tau}\big(M_{\mathrm{H}}^{l+1} - f_{\mathrm{H}}^{l+1}\big), \tag{34a}$$

$$\frac{f_{\mathrm{L}}^{l+1} - f_{\mathrm{L}}^{l}}{\Delta t} = \frac{1}{\tau}\big(Q_{\mathrm{L}}^{l} - \beta\big(M_{\mathrm{L}}^{l} - f_{\mathrm{L}}^{l}\big)\big) + \frac{\beta}{\tau}\big(M_{\mathrm{L}}^{l+1} - f_{\mathrm{L}}^{l+1}\big), \tag{34b}$$

where $\beta = O(1)$.

Theorem 5.1. *This scheme yields the following behavior at: $O\left(\frac{1}{\varepsilon}\right)$ and $O\left(\frac{1}{\varepsilon^2}\right)$.*

- *at $\tau = O\left(\frac{1}{\varepsilon}\right)$, the scheme is first order consistent to $\partial_t f_{\mathrm{H}} = Q_{\mathrm{H}}$, and f_{L}^{l} is an $O(\varepsilon)$ approximation of $\overline{M}_{\mathrm{L}}$;*
- *at $\tau = O\left(\frac{1}{\varepsilon^2}\right)$, both f_{H}^{l} and f_{L}^{l} are within $O(\varepsilon)$ of the unified Maxwellians $\overline{M}_{\mathrm{H}}$ and $\overline{M}_{\mathrm{L}}$, respectively.*

Proof. To prove the second statement:
At this time scale, $\tau = O(\varepsilon^2)$, the system turns out to be:

$$\begin{cases} \partial_t f_{\mathrm{H}} = \dfrac{1}{\varepsilon} Q_{\mathrm{H}}, \\ \partial_t f_{\mathrm{L}} = \dfrac{1}{\varepsilon^2} Q_{\mathrm{L}}. \end{cases}$$

By the same arguments as in the previous sections, one gets:

$$\begin{cases} f_{\mathrm{H}}^{l} - \overline{M}_{\mathrm{H}}^{l} &= O(\varepsilon), \\ f_{\mathrm{L}}^{l} - \overline{M}_{\mathrm{L}}^{l} &= O(\varepsilon^2). \end{cases}$$

for l large enough.
To prove the first statement:
At this time scale, $\tau = O(\varepsilon)$, system (33) can be written as:

$$\begin{cases} \partial_t f_{\mathrm{H}} = Q_{\mathrm{H}}, \\ \partial_t f_{\mathrm{L}} = \dfrac{1}{\varepsilon} Q_{\mathrm{L}}. \end{cases}$$

The scheme still gives $f_{\mathrm{L}}^l \to \overline{M}_{\mathrm{L}}^l$. One just needs to show that the scheme gives a correct discretization of the equation for f_{H} too. Write (5.4a) as (set $\tau = \varepsilon$):

$$\frac{f_{\mathrm{H}}^{l+1} - f_{\mathrm{H}}^l}{\Delta t} = Q_{\mathrm{H}}^l - \beta\big(M_{\mathrm{H}}^l - f_{\mathrm{H}}^l\big) + \beta\big(M_{\mathrm{H}}^{l+1} - f_{\mathrm{H}}^{l+1}\big).$$

Rearrange it, one gets:

$$\frac{f_{\mathrm{H}}^{l+1} - f_{\mathrm{H}}^l}{\Delta t} = Q_{\mathrm{H}}^l - \frac{\beta\Delta t}{1+\beta\Delta t} Q_{\mathrm{H}}^l + \frac{\beta}{1+\beta\Delta t}\big(M_{\mathrm{H}}^{l+1} - M_{\mathrm{H}}^l\big).$$

The second and the third terms on the right are both of order Δt, that is, the scheme gives a first order discretization to $\partial_t f_{\mathrm{H}} = Q_{\mathrm{H}}$.

■

VI. NUMERICAL EXAMPLES

For comparison, the examples chosen are similar to those in [17]. We also perturb the data on the level of macroscopic quantities. For all the examples later: when ε is not very small, so that solving the Boltzmann equation is still possible using the basic explicit scheme with a resolved mesh, we compare our numerical results to those of the forward Euler, and when ε is unbearably small for the forward Euler, we compare our results to its Euler limit. To solve the Euler equations, we used the CLAWPACK Euler solver [41].

A. A Stationary Shock

In this example, we show numerical solution to a Riemann problem of two species. The analytical solution to the Euler equations is a stationary shock. Here, the subscripts 1 and 2 stand for different species.

$$\begin{cases} m_1 = 1, m_2 = 1.5, n_1 = n_2 = 1, u_1 = 1.8, u_2 = 1.3, T_1 = 0.3, T_2 = 0.35, & \text{if } x < 0; \\ m_1 = 1, m_2 = 1.5, n_1 = n_2 = 1.401869, u_1 = u_2 = 1.07, T_1 = T_2 = 0.8605, & \text{if } x > 0. \end{cases}$$

The initial distribution for f is given by summation of two Gaussian functions, so it is far away from the unified Maxwellian $\overline{M}$:

$$f(t=0) = \sum_{i=1}^{2} A_i e^{-B_i(v-C_i)^2}, \tag{35}$$

where

$$B_1 = B_2 = \frac{\rho}{4E - 2\rho u^2(1+\kappa^2)},\ A_1 = A_2 = \frac{n}{2}\sqrt{\frac{B_1}{\pi}},\ \text{and } C_1 - u = u - C_2 = \kappa u, \tag{36}$$

That is, the two Gaussian functions have the same height and variation, but their centers are $2\kappa u$ away from each other. In the numerical experiment, we choose $\kappa = 0.2$, $\Delta x = 10^{-2}$ and Δt is chosen to satisfy the CFL condition: 10^{-3} in our simulation. Numerically, we check whether the scheme gives the Euler limit when ε goes to zero; and whether it matches well with the forward

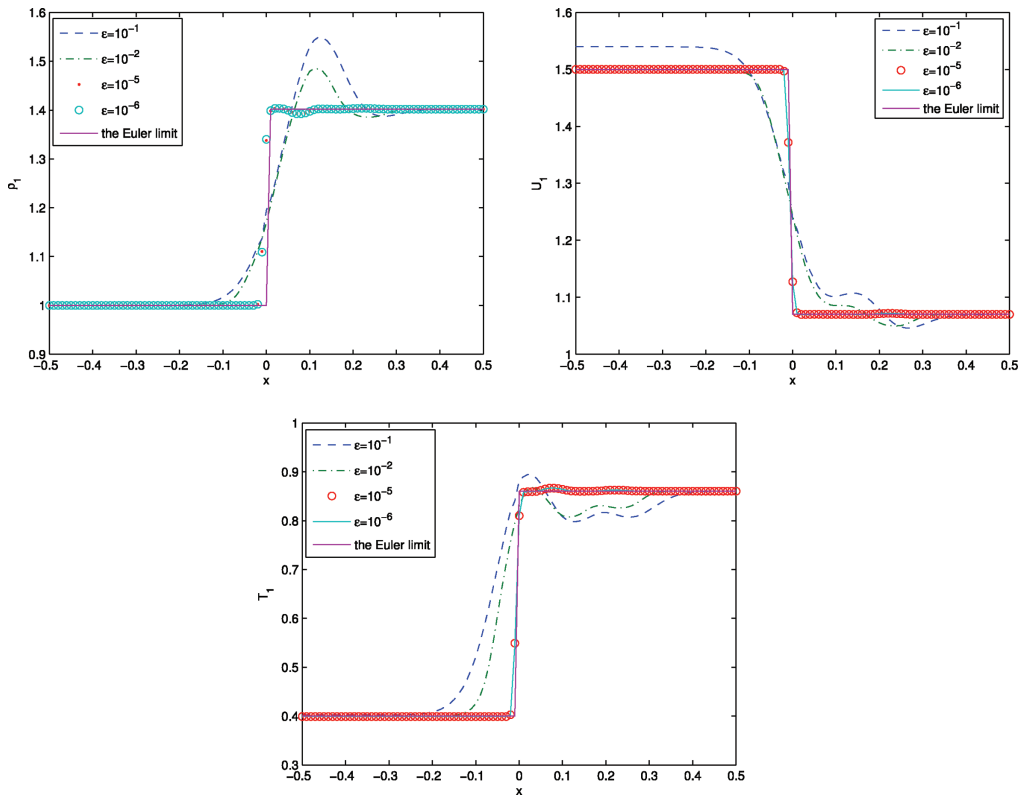

FIG. 2. The stationary shock problem. As $\varepsilon \to 0$, solution of the Boltzmann equation goes to the Euler limit. $t = 0.1$. [Color figure can be viewed in the online issue, which is available at wileyonlinelibrary.com.]

Euler method with relatively fine mesh when ε is big. We first show in Fig. 2 that as ε goes to zero, the numerical solution converges to the Euler limit, the stationary shock in this case. In Fig. 3, we show that the AP scheme matches very well with the numerical results given by the forward Euler method for $\varepsilon = 10^{-1}$. Then, we show in Fig. 4, that given an initial data far away from the unified Maxwellian $\overline{M}$, f gets close to $\overline{M}$ quickly with $\varepsilon = 10^{-5}$. This verifies that the scheme is relaxed-AP numerically. Figure 5 shows that smaller ε gives faster convergence to the equilibria for macroscopic quantities.

B. A Sod Problem

In this example, we solve a Sod problem. The initial data are given by:

$$\begin{cases} m_1 = m_2 = 1, n_1 = 1, n_2 = 1.2, u_1 = 0.6, u_2 = -0.5, T_1 = T_2 = 0.709, & \text{if } x < 0; \\ m_1 = m_2 = 1, n_1 = 0.125, n_2 = 0.2, u_1 = -0.2, u_2 = 0.125, T_1 = T_2 = 0.075, & \text{if } x > 0. \end{cases}$$

The initial distribution is also given by (35) and (36) with $\kappa = 0.2$. For all ε, we choose $\Delta x = 10^{-2}$ and $\Delta t = 10^{-3}$. In this problem, $m_1 = m_2$, so we first show the numerical indifferentiability in Fig. 6, that is: computing the problem as a multispecies system gives the same result as computing

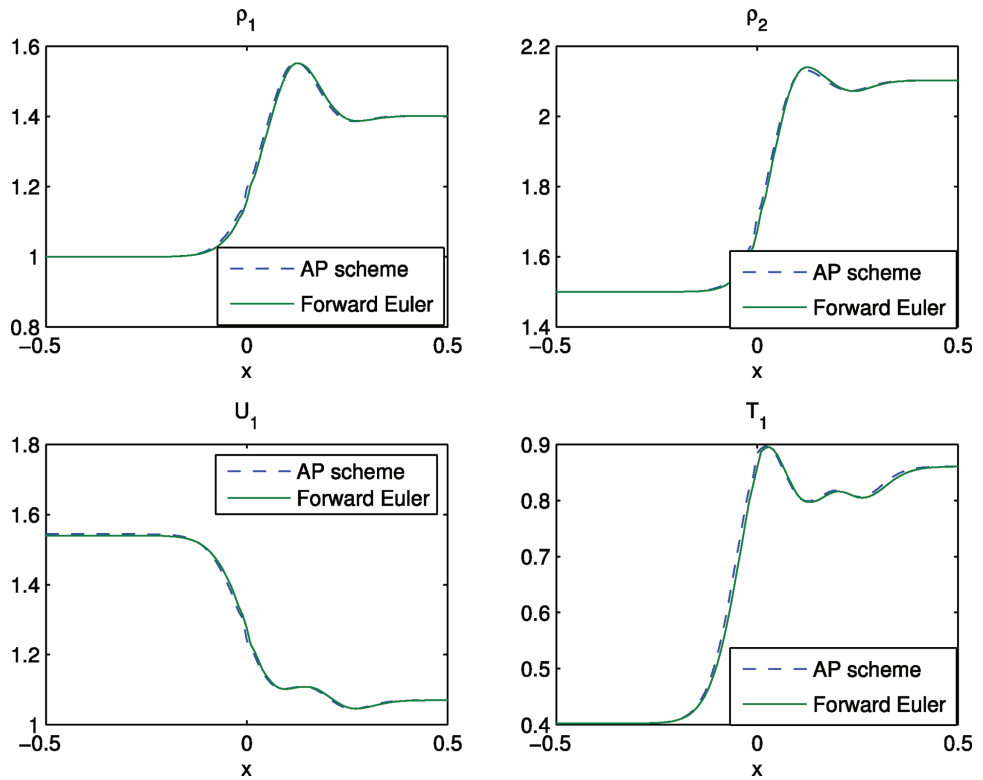

FIG. 3. The stationary shock problem. $\varepsilon = 0.1$ and $t = 0.1$. The dashed line is given by the AP scheme, and the solid line is given by the forward Euler with a fine mesh: $\Delta x = 0.01$ and $\Delta t = 0.0005$. [Color figure can be viewed in the online issue, which is available at wileyonlinelibrary.com.]

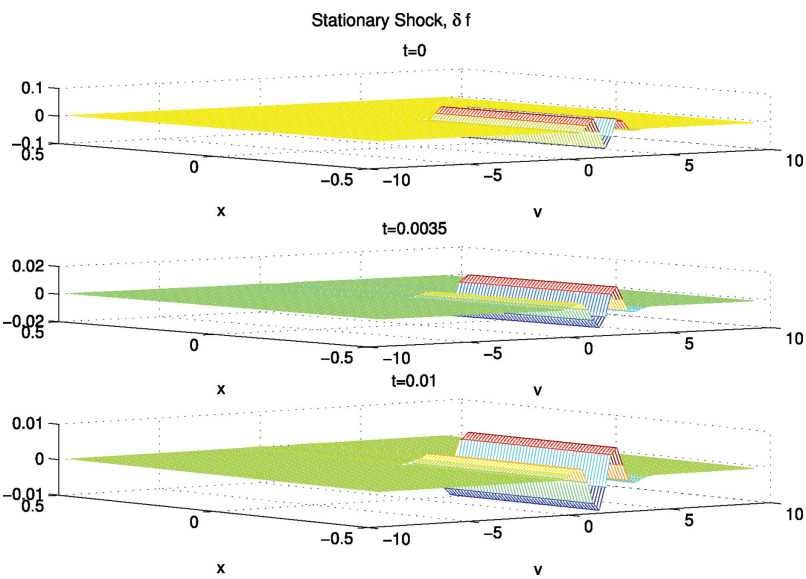

FIG. 4. The stationary shock problem. $\varepsilon = 10^{-5}$, $\delta f = f_1 - \overline{M}_1$ diminishes as time evolves. [Color figure can be viewed in the online issue, which is available at wileyonlinelibrary.com.]

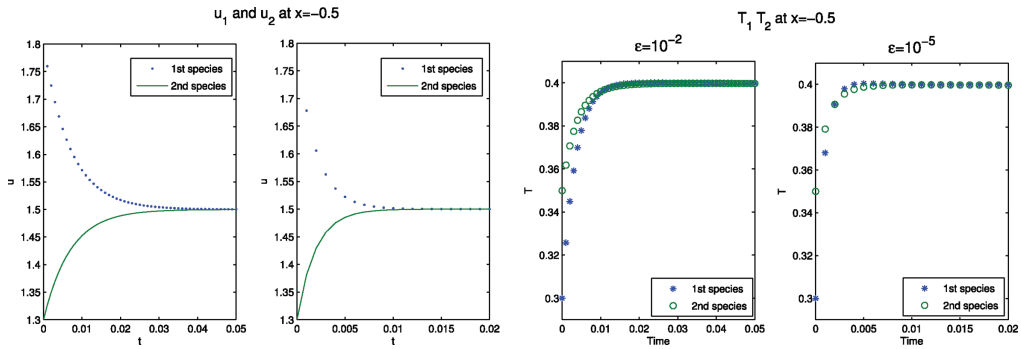

FIG. 5. The stationary shock problem. u_1 and u_2 at $x = -0.5$ on the left and T_1 and T_2 on the right, as functions of time, for $\varepsilon = 10^{-2}$ and 10^{-5}, respectively. Note the different time scales for the two figures. [Color figure can be viewed in the online issue, which is available at wileyonlinelibrary.com.]

the monospecies Boltzmann equation. In Fig. 7, we show that as ε goes to zero, the numerical solution converges to the Euler limit. For ε as big as 10^{-1} and 10^{-2}, we compare the results with those of the forward Euler with a fine mesh. They match well as shown in Fig. 8. In Fig. 9, we show that for $\varepsilon = 10^{-4}$, although the initial f is far away from the unified Maxwellian $\overline{M}$, as time evolves, it converges to $\overline{M}$. This numerically verifies the relaxed-AP property. In Fig. 10, we show the evolution of u with different ε. Apparently different species gradually share the same velocity, and the smaller ε is, the faster the convergence is.

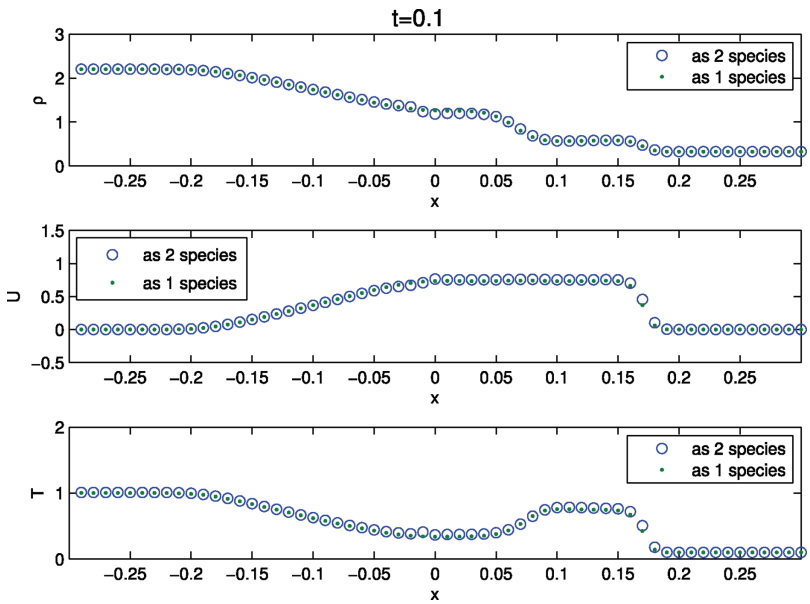

FIG. 6. The Sod problem. Indifferentiability. $t = 0.1$. ρ, u, and T are computed using two species model ("o") and one species model (".."). [Color figure can be viewed in the online issue, which is available at wileyonlinelibrary.com.]

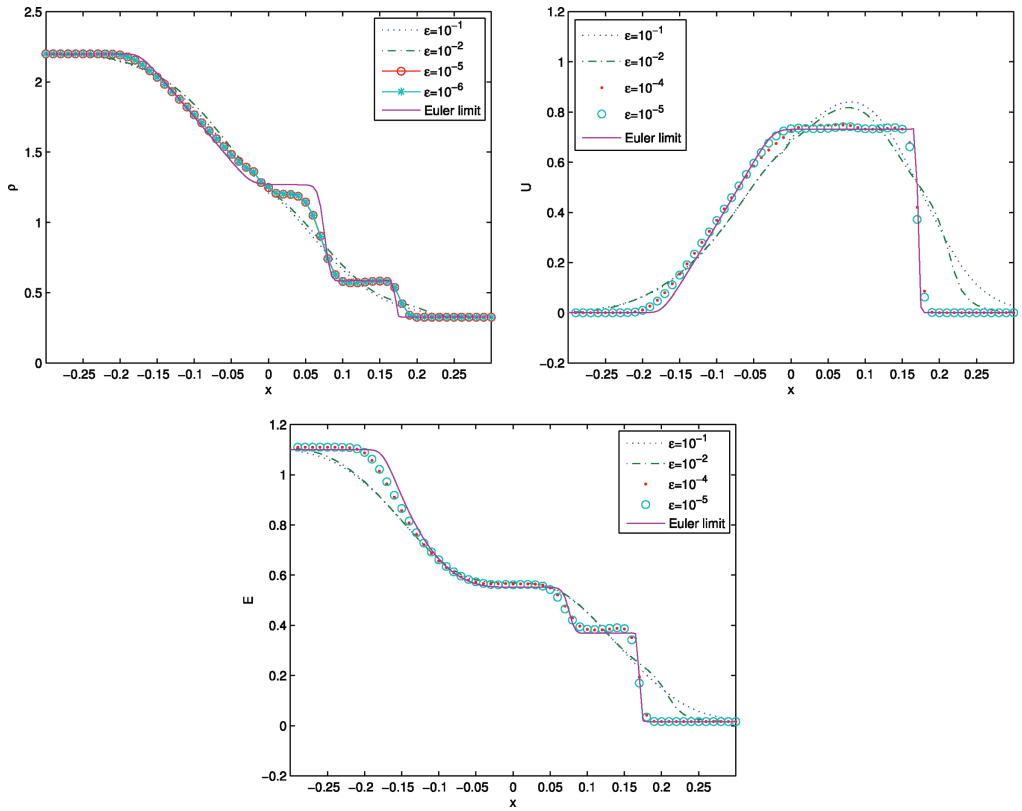

FIG. 7. The Sod problem. $t = 0.1$. As $\varepsilon \to 0$, the numerical results go to the Euler limit. Solid lines give the Euler limit computed using [41]. [Color figure can be viewed in the online issue, which is available at wileyonlinelibrary.com.]

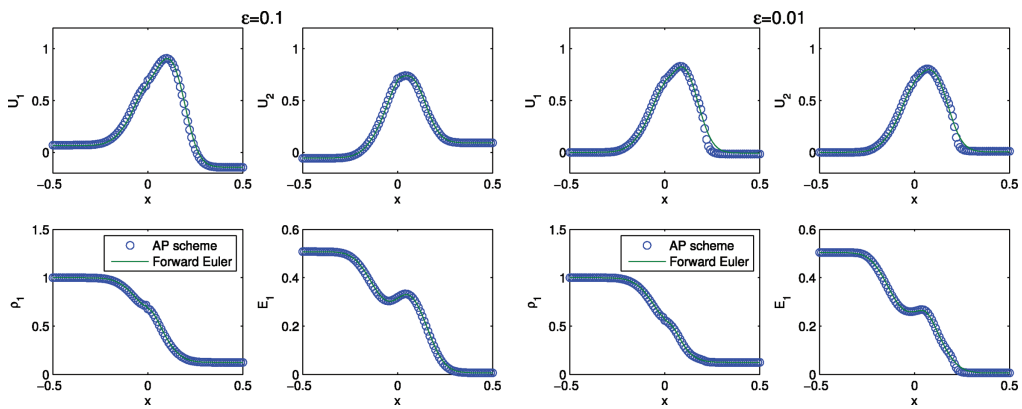

FIG. 8. The Sod problem. $t = 0.1$. For $\varepsilon = 0.1$ and 0.01, we compare the results of the AP scheme, given by the circled lines, and the results of the forward Euler with a fine mesh, given by the solid lines. [Color figure can be viewed in the online issue, which is available at wileyonlinelibrary.com.]

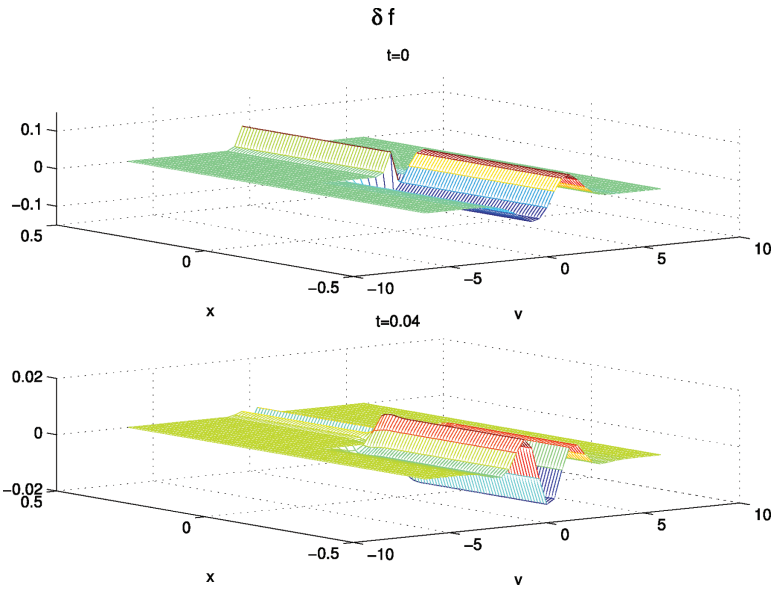

FIG. 9. The Sod problem. $\varepsilon = 10^{-4}$ and $\delta f = f_1 - \overline{M}_1$. [Color figure can be viewed in the online issue, which is available at wileyonlinelibrary.com.]

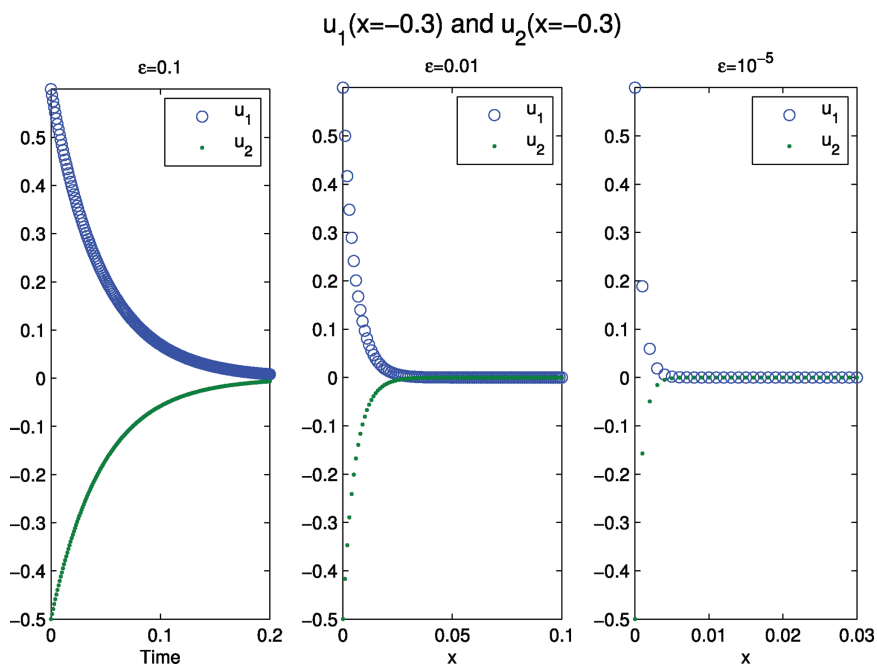

FIG. 10. The Sod problem. The three figures show velocities u_1 and u_2 at $x = -0.3$ as functions of time for $\varepsilon = 0.1, 0.01,$ and 10^{-5}. Note different time scales for three figures. [Color figure can be viewed in the online issue, which is available at wileyonlinelibrary.com.]

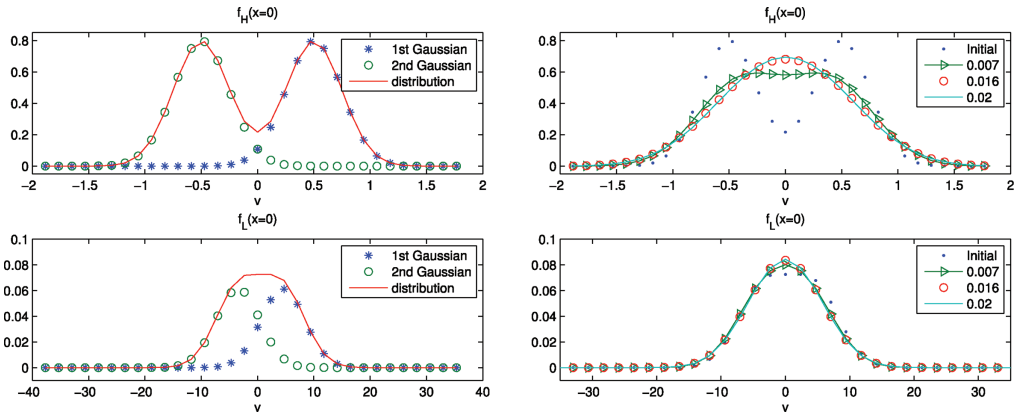

FIG. 11. The disparate masses problem. The left figure shows the initial distributions, and the right figure shows the time evolutions of f_{H} and f_{L}. f_{H} is put at the top, and f_{L} is at the bottom. At $t = 0.007$, f_{L} is close to $\overline{M}_{\mathrm{L}}$, whereas f_{H} is still far away from the equilibrium. Note the different scales for v. [Color figure can be viewed in the online issue, which is available at wileyonlinelibrary.com.]

C. A Disparate Masses Problem

In this example, we solve the disparate masses system. Define $\varepsilon = \sqrt{\frac{m_{\mathrm{L}}}{m_{\mathrm{H}}}}$, we want to verify that the light species gets close to the unified Maxwellian $\overline{M}_{\mathrm{L}}$ faster than the heavy one. We solve an inhomogeneous problem with the following initial data:

$$m_{\mathrm{H}} = 8, \quad m_{\mathrm{L}} = 0.08, \quad u_{\mathrm{H}} = 0, \quad u_{\mathrm{L}} = 0.5, \quad T_{\mathrm{H}} = T_{\mathrm{L}} = 2.5, \quad n_{\mathrm{H}} = 1, \quad \text{and} \quad n_{\mathrm{L}} = 1.2.$$

The initial distribution functions are still given by the summation of two Gaussians as in (35), with parameters $A_1 = A_2$ and $B_1 = B_2$ defined in (36), and C_1 and C_2 defined by: $C_1 - u = u - C_2 = \kappa$. We choose $\kappa = 0.5$ for the heavy species and $\kappa = 4$ for the light one. In Fig. 11, on the left we show the initial distribution functions for the two species, both of which are given by summation of two Gaussian functions and are far away from the Maxwellian. On the right, we show several snapshots of the distribution functions as they evolve. In Fig. 12, we show that as time evolves, the velocities converge toward each other. Note that the heavy species weighted more when computing for the mean velocity $\bar{u}$ as in (5b), thus its average velocity does not change much.

VII. CONCLUSIONS

Motivated by the work of Filbet–Jin [12], we use an appropriate BGK operator that is defined by the common velocity and common temperature to penalize the stiff collision operator for multispecies Boltzmann equation, which yields an AP scheme. This scheme can capture the Euler limit with mesh size and time step independent of the Knudsen number, thus it is suitable for simulating the multispecies Boltzmann equation efficiently in both the kinetic and fluid regimes. The BGK penalization allows one to avoid inverting the nonlinear Boltzmann collision operator in the fluid regime. This approach is also applied to system of gas mixture with disparate masses. Numerical results were used to demonstrate the validity of the scheme.

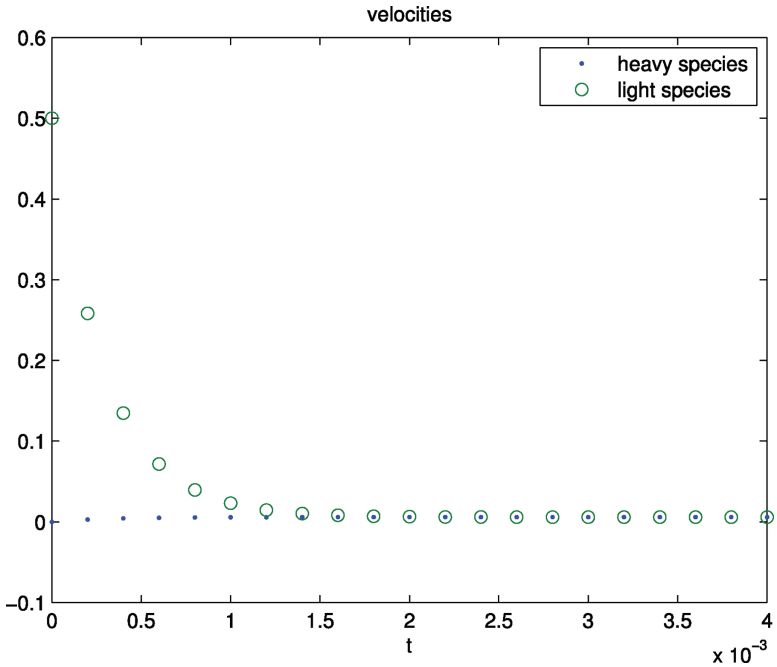

FIG. 12. The disparate masses problem. The velocities for the two species converge to each other. [Color figure can be viewed in the online issue, which is available at wileyonlinelibrary.com.]

In the future, we will extend and verify numerically this method to the case of more general collision kernels and in higher space dimension.

The second author thanks Dr. Cory Hauck and Dr. Bokai Yan for stimulating discussions and the referee for suggesting many improvements.

References

1. C. Besse, S. Borghol, T. Goudon, I. Lacroix-Violet, and J.-P. Dudon, Hydrodynamic regimes, Knudsen layer, numerical schemes: Definition of boundary fluxes, Adv Appl Math Mech 3 (2011), 519–561.
2. J. F. Bourgat, P. Le Tallec, B. Perthame, and Y. Qiu, Coupling Boltzmann and Euler equations without overlapping, A. Quarteroni, J. Périaux, Y. A. Kuznetsov, and O. Widlund, editors, Domain decomposition methods in science and engineering, AMS, Providence, RI, 1994, pp. 377–398.
3. P. Degond and S. Jin, A smooth transition model between kinetic and diffusion equations, SIAM J Numer Anal 42 (2005), 2671–2687.
4. P. Degond, S. Jin, and L. Mieussens, A smooth transition model between kinetic and hydrodynamic equations, J Comput Phys 209 (2005), 665–694.
5. F. Golse, S. Jin, and C. D. Levermore, A domain decomposition analysis for a two-scale linear transport problem, Math Model Numer Anal 37 (2002), 869–892.
6. M. Guenther, J. Struckmeier, P. Le Tallec, and J. Perlat, Numerical modeling of gas flows in the transition between rarefied and continuu regimes, Notes Numer Fluid Mech 66 (1998), 222–241.
7. S. Jin, X. Yang, and G. Yuan, A domain decomposition method for a two-scale transport equation with energy flux conserved at the interface, Kinetic Relat Models 1 (2008), 65–84.

8. A. Klar, H. Neunzert, and J. Struckmeier, Transition from kinetic theory to macroscopic fluid equations: a problem for domain decomposition and a source for new algorithms, Transp Theory Stat Phys 29 (2000), 93–106.
9. P. Le Tallec and F. Mallinger, Coupling Boltzmann and Navier-Stokes equations by half fluxes, J Comput Phys 136 (1997), 51–67.
10. A. F. Vasseur, Rigorous derivation of the kinetic/fluid coupling involving a kinetic layer on a toy problem, ARMA, to appear.
11. S. Jin, Efficient asymptotic-preserving (AP) schemes for some multiscale kinetic equations, SIAM J Sci Comp 21 (1999), 441–454.
12. F. Filbet and S. Jin, A class of asymptotic-preserving schemes for kinetic equations and related problems with stiff sources, J Comput Phys 229 (2010), 7625–7648.
13. S. Jin, Asymptotic preserving (AP) schemes for multiscale kinetic and hyperbolic equations: a review, Lecture Notes for Summer School on "Methods and Models of Kinetic Theory" (M&MKT), Porto Ercole, Grosseto, Italy, June 2010.
14. S. Jin, Runge-Kutta methods for hyperbolic conservation laws with stiff relaxation terms, J Comput Phys 122 (1995), 51–67.
15. R. Caflisch, S. Jin, and G. Russo, Uniformly accurate schemes for hyperbolic systems with relaxations, SIAM J Numer Anal 34 (1997), 246–281.
16. M. Lemou and L. Mieussens, A new asymptotic preserving scheme based on micro–macro formulation for linear kinetic equations in the diffusion limit, SIAM J Sci Comput 31 (2008), 334–368.
17. S. Jin and Y. Shi, A micro-macro decomposition-based asymptotic-preserving scheme for the multispecies Boltzmann equation, SIAM J Sci Comput 31 (2010), 4580–4606.
18. E. Gabetta, L. Pareschi, and G. Toscani, Relaxation schemes for nonlinear kinetic equations, SIAM J Numer Anal 34 (1997), 2168–2194.
19. F. Coron and B. Perthame, Numerical passage from kinetic to fluid equations, SIAM J Numer Anal 28 (1991), 26–42.
20. B. Yan and S. Jin, A successive penalty-based asymptotic-preserving scheme for kinetic equations, preprint.
21. G. Dimarco and L. Pareschi, Exponential Runge–Kutta methods for stiff kinetic equations, SIAM J Numer Anal 49 (2011), 2057–2077.
22. F. Filbet and A. Rambaud, Analysis of an asymptotic preserving scheme for relaxation systems, 2011. arXiv:1105.2655.
23. S. Jin and B. Yan, A class of asymptotic-preserving schemes for the Fokker-Planck-Landau equation, J Comp Phys 230 (2011), 6420–6437.
24. F. Filbet, J. Hu, and S. Jin, A numerical scheme for the quantum Boltzmann equation efficient in the fluid regime, Math Model Numer Anal 46 (2012), 443–463.
25. J. Hu, S. Jin, and B. Yan, A numerical scheme for the quantum Fokker-Planck-Landau equation efficient in the fluid regime, Commun Comp Phys 12 (2012), 1541–1561.
26. H. Grad, F. Devienne, editor, Rarefied gas dynamics, Pergamon, London, England, 1960, pp. 10–138.
27. S. I. Braginskii, Transport processes in a plasma, Rev Plasma Phys 1 (1965), 205.
28. L. Spitzer and R. Härm, Transport phenomena in a completely ionized gas, Phys Rev 89 (1953), 977–981.
29. F. Charles and L. Desvillettes, Small mass ratio limit of Boltzmann equations in the context of the study of evolution of dust particles in a rarefied atmosphere, J Stat Phys 137 (2009), 539–567.
30. J. H. Ferziger and H. G. Kaper, Mathematical theory of transport processes in gases, North-Holland Pub. Co, Amsterdam, 1972.
31. E. Goldman and L. Sirovich, Equations for gas mixtures, Phys Fluids 10 (1967), 1928–1940.

32. P. Andries, K. Aoki, and B. Perthame, A consistent BGK-type model for gas mixtures, J Stat Phys 106 (2002), 993–1018.

33. V. Garzò, A. Santos, and J. J. Brey, A kinetic model for a multicomponent gas, Phys Fluids 1 (1989), 380–384.

34. E. P. Gross and M. Krook, Model for collision processes in gases: small-amplitude oscillations of charged two-component systems, Phys Rev 102 (1956), 593–604.

35. L. Pareschi and G. Russo, Numerical solution of the Boltzmann equation I: spectrally accurate approximation of the collision operator, SIAM J Numer Anal 37 (2000), 1217–1245.

36. R. J. LeVeque, Numerical methods for conservation laws, Lectures in mathematics ETH Zürich, Birkhäuser Verlag, 1992.

37. R. M. Chmieleski and J. H. Ferziger, Transport properties of a nonequilibrium partially ionized gas, Phys Fluids 10 (1967), 364–371.

38. E. A. Johnson, Energy and momentum equations for disparate-mass binary gases, Phys Fluids 16 (1973), 45–49.

39. P. Degond and B. Lucquin-Desreux, The asymptotics of collision operators for two species of particles of disparate masses, Math Models Methods Appl Sci 6 (1996), 405–436.

40. P. Degond and B. Lucquin-Desreux, Transport coefficients of plasmas and disparate mass binary gases, Transp Theory Stat Phys 25 (1996), 595–633.

41. http://depts.washington.edu/clawpack/clawpack-4.3/.